

GNSS-grade space atomic frequency standards: Current status and ongoing developments

Etienne Batori*, Nil Almat, Christoph Affolderbach, Gaetano Mileti*

Laboratoire Temps – Fréquence (LTF), Institut de Physique, Université de Neuchâtel, 2000 Neuchâtel, Switzerland

Received 8 April 2020; received in revised form 4 September 2020; accepted 5 September 2020

Available online 18 September 2020

Abstract

We present an overview on the current state of Global Navigation Satellite Systems (GNSS)-grade or better space atomic frequency standards' (SAFS) technologies and discuss their applications. We estimate that a total of more than 1000 such standards were sent to space so far, the vast majority consisting of rubidium-cell frequency standards, Cs atomic beam frequency standards, and passive hydrogen masers. Finally, we review a variety of ongoing developments in view of future new generations of GNSS-grade SAFSs.

© 2020 COSPAR. Published by Elsevier Ltd. This is an open access article under the CC BY license (<http://creativecommons.org/licenses/by/4.0/>).

Keywords: Space atomic frequency standards; GNSS; RAFS; Hydrogen maser; Cesium beam

1. Introduction

Since the first demonstration of an atomic frequency standard (AFS) (Essen and Parry, 1955) and the following redefinition of the SI second in 1967, AFSs have found a multitude of applications (Maleki and Prestage, 2005), both on ground as well as in space.

Primary frequency standards directly interrogate the unperturbed Cesium (Cs) 133 ground state hyperfine transition whose frequency of 9.192631770 GHz corresponds to the definition of the second in the SI system and should have undergone an accuracy evaluation (Riehle, 2003). Laser-cooled Cs fountain primary frequency standards - as operated in national metrology institutes - represent a tiny proportion of the total number of AFSs (Wynands and Weyers, 2005). They are the successors of the early primary Cs hot beam frequency standards (Bauch, 2003). Note that a small number of certain non-Cs frequency standards realizing the secondary representation of the sec-

ond (Riehle et al., 2018) are considered being traceable to the primary Cs AFS, such as rubidium (Rb) fountains (Gill, 2005; Peil et al., 2017). These AFS are mainly employed in metrology and timekeeping applications on ground by national metrology institutes and in fundamental or industrial metrology applications.

Other AFSs either interrogate a different frequency reference or a Cs reference without full accuracy evaluation of its frequency bias. Examples are AFSs based on other alkali atoms microwave transitions, trapped-ion microwave transitions (Gill et al., 2003), optical clocks (Ludlow et al., 2015), Cs vapor-cell and commercial Cs hot beams (Microsemi, 2020). For many space and ground (Akiyama et al., 2019) applications, such AFSs with good long-term frequency stability are sufficient and accuracy of the frequency output is generally not required.

Most industrial and space-oriented developments focused on the “classical three” (Vanier and Tomescu, 2015) atomic frequency standards: the thermal Cs beam, the hydrogen (H) maser (H-maser) (passive or active) and the Rb atomic frequency standard (RAFS). It is therefore no surprise that so far almost all space AFS (SAFS) ever sent into orbit or deep space are of one of these kinds.

* Corresponding authors.

E-mail addresses: etienne.batori@unine.ch (E. Batori), gaetano.mileti@unine.ch (G. Mileti).

SAFSs' and ground AFSs' qualifications differ. First, the former generally need to be smaller, lighter and consume less energy than the latter. Second, aside from being compatible with the absence of (or controlled) atmosphere, SAFSs must be launch-resilient, radiation hard with respect to ionizing radiation in space and reliable for the whole mission's duration. In addition, Global Navigation Satellite Systems (GNSS) grade SAFSs are generally required to achieve high stability performance on the level of 10^{-14} over one day (Droz et al., 2009).

To our knowledge, the most recent review on GNSS-grade SAFS was presented 14 years ago by (Mallette et al., 2006). Updated reviews on the development status of different GNSS were published in 2010 and 2012 by the same authors (Mallette et al., 2012, 2010), however without detailed data on the number of GNSS-grade SAFS flown. In (Mallette et al., 2006) it was estimated that at least 452 GNSS-grade SAFS had been sent to orbit or deep space compared to 300 in 1996 (Bhaskar et al., 1996).

In this publication, we aim to give an updated overview on the numbers and types of GNSS-grade or better SAFS sent to space so far or under on-going development. Section 2 will give an overview of the currently existing established SAFSs technologies. In Section 3 we describe the main applications of SAFSs with an emphasis on GNSS. Section 4 will estimate the number of GNSS-grade or better SAFSs sent into orbit and deep space so far. Section 5 will review some recent or on-going developments relevant for next generations of SAFSs.

2. Current SAFS technologies

2.1. The RAFS

The RAFS was the first frequency standard to be tested in a suborbital flight in 1961 (Bhaskar et al., 1996). It is also the first SAFS placed in orbit in the NTS-1 satellite in the early days of the Global Positioning System (GPS) in 1974 (McCaskill and Buisson, 1975). RAFS is also the first and only SAFS having been sent into deep space for the Cassini-Huygens mission in 1977. The two RAFS units sent were necessary to achieve sufficiently stable communication between the receiver and transmitter during the Doppler wind experiment descent time (Bird et al., 1997).

The RAFS (Camparo, 2007) physics package consist of ^{87}Rb -filled glass cell placed in a microwave cavity tuned near the 6.834 GHz Rb ground-state hyperfine transition frequency. The $F = 2$ ground state level is populated by a discharge lamp's radiation after passing through a ^{85}Rb filtering cell. A control loop tunes the microwave frequency such that the light transmission signal through the Rb cell detected by a photodiode is minimized. This configuration is known as the separated filter technique (SFT) (Mei et al., 2016), as opposed to the integrated filter technique (IFT) (Rochat et al., 1994). In both cases, the atoms are interrogated in a continuous-wave double-resonance scheme

(CW-DR) where the optical and microwave radiations are applied simultaneously to the atoms.

Still today, a primary interest in RAFS comes from its low volume, low cost and low power consumption compared to the Cs beam and H-maser standards. Its simple design is also particularly suited for miniaturization (Vanier and Tomescu, 2015). Furthermore, atoms in RAFS do not consume themselves rapidly, unlike Cs and H atoms in Cs beams and H-masers, which in principle is advantageous for the instrument lifetime.

The performance limitations of RAFS are to be separated between short (1 s to 10^4 s) and long-term stabilities. The short-term stability is generally limited by the quality factor (Q_j) of the atomic resonance signal and its signal-to-noise ratio (SNR). The long-term stability limits arise from frequency biases that can vary in time in response to external or operational parameters acting on the AFS. An early example is the satellite's temperature oscillations (McCaskill and Buisson, 1975). One of today's "most problematic" shifts is the light shift making the atomic reference frequency vary in response to variations in the frequency or intensity of the pump light source (Formichella et al., 2017).

Today's space RAFSs' basic design and operation mode remain largely unaltered. Furthermore, recent and future developments for the Chinese GNSS (BeiDou) (Mei et al., 2016) and the Indian Regional Navigation Satellite System (IRNSS) (Bandi et al., 2019) still feature this mature technology.

2.2. The cesium beam frequency standard

Soon after the redefinition of the second in 1967, four Cs beam atomic standards flew on commercial airplane flights around the earth in the so-called "Hafele-Keating experiment" to demonstrate the theory of relativity effects on clocks flying around the world in opposite directions (Hafele and Keating, 1972). A few years later, the first two Cs beam frequency standards were sent into orbit in 1977 in the NTS-2 satellite (Bhaskar et al., 1996). Since then, dozens of them have been regularly sent to space in the Russian Global Navigation Satellite System (GLO-NASS) and GPS satellites (Mallette et al., 2006).

In the physics package of a Cs beam AFS, a thermal beam of ^{133}Cs atoms is generated by an oven. Magnetic state deflectors select the atoms in the $|F = 4, m_F = 0\rangle$ at omic ground state. The beam passes in a so-called Ramsey cavity whose two arms will excite the atoms twice with the microwave transition, according to Ramsey's method of separated oscillating fields (Ramsey, 1990). A second magnetic state selector called the analyzer selects the $|F = 3, m_F = 0\rangle$ states and atoms are detected using a hot wire. The microwave frequency is tuned such that the signal, called Ramsey fringes, is maximized (Vanier and Tomescu, 2015). This interrogation scheme is called a Ramsey scheme and was proposed by (Arditi and Carver, 1964) following (Ramsey, 1956) to improve the transition's

quality factor and hence reduce the short-term instabilities' level.

Interest in Cs frequency standards come from the wide availability of Cs on earth as well as its low melting point (Vanier and Audoin, 2005). Compared to their cell-type counterparts (RAFS or H-maser), they show small long-term frequency drifts and can thus reach excellent long-term stability (Microsemi, 2020). These advantages come however at the price of a relatively complex vacuum chamber to be maintained for the atomic beam.

The short-term stability is limited by the detection shot noise. For the Cs frequency standards featuring magnetic selectors the mainly time-varying frequency biases affecting the long-term stability are “the magnetic field and its homogeneity, the second-order Doppler effect, and the cavity phase shifts” (Vanier and Tomescu, 2015).

2.3. The hydrogen maser

The first (Bhaskar et al., 1996) H-maser (active) was sent into space in 1976 for less than 2 h in the framework of the “Gravity Probe A experiment” (Vessot et al., 1980). In 1996, the H-maser technology was seen as “uniquely suited for testing the fundamental physics laws” (Bhaskar et al., 1996). The European GNSS (GALILEO) GIOVE-B technology validation satellite including the first orbiting H-maser (passive) changed this perspective (Waller et al., 2009). Since then, as it is presented in Section 3.1 and figure Fig. 2, many GALILEO and BeiDou satellites including passive H-masers were sent into orbit. Vremya-CH is building a passive space-grade H-maser that is very likely to be seen in GLONASS in the future (Belyaev et al., 2019). Vremya-CH also built the first continuously orbiting active H-masers sent within the Radioastron satellite launched in 2011 (Belyaev et al., 2019; Utkin et al., 2012).

The active H-maser is different from that of the two other classic AFS types in the sense that no microwave probing power is needed to interrogate the 1420.405 MHz ground state hyperfine microwave frequency. Molecular hydrogen from a reservoir is dissociated to hydrogen atoms and formed to an atomic beam. By means of a magnetic state selector only higher energy atoms with $F = 1$, $m_F = 0, 1$ are streamed into a bulb placed inside a microwave cavity with sufficiently high quality factor so that self-sustained oscillations due to stimulated emission occur. This detected signal is used to stabilize the frequency of a crystal oscillator (Vanier and Tomescu, 2015). Constraints such as high quality factor or cavity mode homogeneity makes this particular device more difficult to build than the passive H-maser. In that case, the H atoms are used as an amplifier of a microwave input frequency.

In its active form, the H-maser is one of the most stable SAFS. However, due to constraints regarding the cavity quality factor resulting in a voluminous, heavy and high power device, its usage has been restricted to ground and fundamental space applications. The passive form is how-

ever more prone to miniaturization with a compromise on the frequency's stability (Vanier and Tomescu, 2015).

2.4. $^{199}\text{Hg}^+$ trapped-ion for DSAC

The Jet Propulsion Laboratory (JPL) mercury trapped-ion ($^{199}\text{Hg}^+$) (Burt et al., 2016; Tjoelker et al., 2016) is one of the few non-classical frequency standards sent into space. Mercury is not only a new atom in space but also is not an alkali atom. The AFS was launched in June 2019 (Georgescu, 2019). There are currently no publications on the operation or performance of this SAFS.

In a mercury trapped-ion AFS, a $^{202}\text{Hg}^+$ discharge lamp is used to prepare and interrogate the ion cloud placed in a first part of an ion trap, which traditionally consist of either combined static electric and magnetic fields (Penning trap) or combined dc and rf electric fields (Paul trap) (Dehmelt, 1990). In order to avoid light shift, the 40.5 GHz hyperfine frequency microwave interaction takes place in a light free area. Thanks to the combination of different electrodes, the ions are shuttled between the two respective regions. These operations consist of up to 50% cycle time resulting to an equivalent cycle dead time (Tjoelker et al., 2016; Vanier and Tomescu, 2015).

Short-term stability is also governed by SNR and transition line quality factor (Tjoelker et al., 2016). The electromagnetic trap technology is less sensitive to external perturbation sources such as wall collisions, magnetic sensitivity and temperature sensitivity resulting in better long-term stability (Seubert et al., 2013).

3. SAFS applications

Applications of high-performance SAFS can be roughly divided into two main categories: In first place, Global Navigation Satellite Systems (GNSS) regroup by far the highest number of SAFS sent into space. As the second category, other and often science-motivated space missions account for a far lesser number of SAFS, but show a richer variety of SAFS in use. In the following, we discuss these two main application categories.

3.1. GNSS

GNSS applications were one of the primary motivations to develop space-borne frequency standards (Bhaskar et al., 1996). First, SAFSs need less frequent time and frequency ground corrections than quartz. Second, according to (Bhaskar et al., 1997) and (Bloch et al., 2002), SAFSs are insensitive to space radiations compared to quartz.

As we will see in Section 4, the vast majority of SAFSs were sent into orbit within the GNSS framework. The reasons for this high number of SAFS are multiple: In the first place, each GNSS system requires an elevated number of satellites to operate. For example, the GALILEO system requires 27 working plus three backup satellites (Droz et al., 2009), with similar requirements for other systems.

In addition, for redundancy several SAFSs are typically flown on each satellite. For example, the BeiDou-2 and BeiDou-3 satellites contain four SAFSs each (Wu et al., 2018). Furthermore, there is an increasing number of different GNSS systems operating or under development, reflecting the wish of several local powers on different continents to use their own systems. Finally, the limited lifetime of each GNSS satellite requires their continuous replacement. Note that in the early days of GNSS, satellites' lifetime were as short as one year (Mallette et al., 2006) whereas GALILEO's current requirements are 12 years lifetime per satellite (Droz et al., 2009).

Past and current lines of development on SAFS on one hand concern the constant search for SAFSs with reduced cost, volume, mass, and power consumption, in order to achieve more cost-effective GNSS satellites and launches. On the other hand, new applications and improvements in positioning accuracy being directly linked to the GNSS satellites' navigation message stability, i.e. a compromise between the SAFSs mid-term stability and the recalibration frequency from the ground segment, are calling for improved clock performances.

In order to illustrate the evolution of the GNSS-grade SAFSs stability from the beginning of GNSS to today, a set of flown SAFSs' Allan deviations are presented Fig. 1.

GNSS also accidentally contributed to fundamental physics within the Galileo gravitational Redshift test with Eccentric sATellites (GREAT) experiment. Here, two satellites that initially had been sent into non-nominal elliptical orbits due to launch problems, finally were exploited to improve the experimental validation of gravitational redshift of Gravity Probe A's (Vessot et al., 1980) by a factor 5.6 (Delva et al., 2019).

The following subsections describe the state of the different GNSSs as of today. For a complete history starting

from the beginning of the GNSS era to 2012, the reader is referred to (Mallette et al., 2006) and (Mallette et al., 2012). A detailed description of the different GNSS systems can be found in (Teunissen and Montenbruck, 2017).

3.1.1. BeiDou

As of July 2020, 55 BeiDou-2 and BeiDou-3 block satellites were launched, completing the BeiDou constellation (BeiDou Navigation Satellite System, 2020). The satellites contain four RAFS for BeiDou-2 or 2 RAFS plus 2 H-masers for BeiDou-3 (Wu et al., 2018; Xu et al., 2019). The H-masers have been built in China (Wu et al., 2018). The RAFS were built by SpectraTime and in China (Huang et al., 2019; Xu et al., 2019).

3.1.2. GALILEO

Apart from the GIOVE-A and GIOVE-B satellites, 26 regular GALILEO satellites were launched so far (European GNSS Agency, 2020). Each of them contains two RAFSs and two passive H-masers.

3.1.3. GLONASS

Between 10 December 2003 and 16 March 2020, we counted 50 reported GLONASS-M satellites (including 6 failed launches) carrying 3 Cs beam clocks each (Betz, 2015). This generation of satellites is not under production anymore and the last GLONASS-M satellite is expected to be launched in 2020. Two GLONASS-K1 satellites – the successor of GLONASS-M – were launched in 2011 and 2014 and contain two Cs beams and two RAFSs each (Betz, 2015; ISS-Reshetnev, 2020).

3.1.4. GPS

A total of 12 IIF satellites were launched, each containing one Cs beam clock and two RAFS (Los Angeles Air Force Base, 2012a). The first three block III satellites containing three RAFSs each (Los Angeles Air Force Base, 2012b) were sent into orbit in 2018, 2019 and 2020.

3.1.5. IRNSS

The IRNSS space segment consists of 9 (including one unsuccessful launch) satellites launched between 2013 and 2018 (Department of Space Indian Space Research Organisation, n.d.). The IRNSS-1A satellite contains three RAFS fabricated by SpectraTime (Thoelert et al., 2014).

3.1.6. QZSS

The Japanese local navigation system quasi-zenith satellite system (QZSS) space segment consists of four satellites launched between 2010 and 2017 (Quasi-Zenith Satellite System, 2020). The QZS-1 satellite has two RAFS on board (Nakamura et al., 2011).

3.2. Other applications

Other applications of SAFSs (Maleki and Prestage, 2005) concern fields such as fundamental physics, astrome-

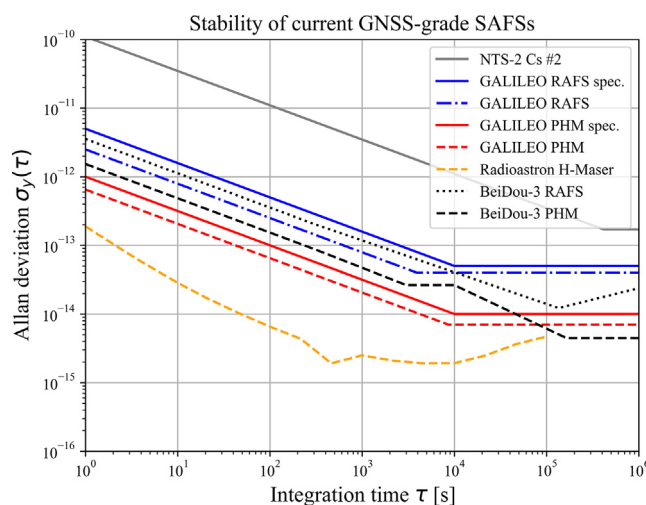


Fig. 1. Allan deviations of different current space clocks. NTS-2 Cs#2 (McCaskill et al., 1978), GALILEO RAFS and PHM specifications and data (Droz et al., 2006; Micalizio et al., 2012), Radioastron (Utkin et al., 2012), BeiDou-3 RAFS and PHM (Guo et al., 2020).

try, time-keeping, deep-space navigation and telecommunications. Although the number of SAFSs used in such applications is not comparable to that of the ones used for GNSS, they can feature more advanced and more stable, yet also heavier, bigger, and more expensive types of clocks.

In the preceding sections, we already mentioned past missions that featured key SAFSs such as the Gravity probe A experiment and the Cassini-Huygens mission. In the following, we discuss a selection of present and future space missions benefiting from AFSs.

3.2.1. Radioastron

The Russian Radioastron radio telescope program began in the 1990s. Its early development included the development of the active hydrogen maser and RAFS manufacture in the Observatoire de Neuchâtel, based on previous RAFS development under ESA programme. Due to lack of budget, the program stopped and only two RAFS were finally built (Couplet et al., 1995; Droz et al., 2009; Rochat et al., 1994). Both technologies were transferred to SpectraTime who is now manufacturing space-grade RAFS, passive H-maser and the active H-maser included in the Atomic Clock Ensemble in Space (ACES) mission (Droz et al., 2009).

Within the Radioastron program, the Spektr-R satellite carrying a 10-m radio telescope was sent into orbit in 2011 flying the two RAFS and the first two active H-masers ever sent into orbit built by Vremya-CH (Kardashev et al., 2013). The mission was officially abandoned in May 2019 due to loss of contact in January 2019 (Astro Space Center, 2019).

3.2.2. GAIA

The European Space Agency (ESA) astrometric satellite is placed in one of the Sun-Earth-Moon Lagrange points. The purpose of the mission is to measure kinematic, dynamic and chemical properties of the Milky Way for a nominal five-year lifetime. It contains one RAFS whose stability of “a few ns for 6 h” (Prusti et al., 2016) is used to accurately attribute time tags to the images. The mission duration was extended in 2018 (European Space Agency, 2018).

3.2.3. ACES

The future ACES ESA mission will, among others, measure the physical constants' time dependency (Laurent et al., 2007). The payload contains two clocks: a laser-cooled Cs beam clock named PHARAO that was developed by SYRTE, LKB, and the French space agency CNES, and a space active H-maser (SHM) developed by SpectraTime (Droz et al., 2009).

PHARAO will make use of the low-gravity condition once installed on the international space station (ISS). The clock will also allow performing improved time transfer and clock comparison on intercontinental scale (Heß et al., 2011).

3.2.4. AEHF

The advance extremely high frequency (AEHF) system is the military strategic and tactical relay satellite (MIL-STAR)'s follow-on mission serving for secure military telecommunication. Since the publication of the previous review by Mallette et al. (Mallette et al., 2006), the 6 satellites were sent into orbit and the constellation was completed 26 March 2020 (Lockheed Martin, 2020).

The satellites contain three Frequency Electronics Inc. (FEI) space RAFSs (FEI, 2013) fulfilling the stability requirements of such secure telecommunication applications (Bhaskar et al., 1997).

3.2.5. Deep space applications

The presence of a SAFS on board a spacecraft allows quicker, more accurate and more efficient positioning by means of the one-way technique instead of the two-way technique (Ely and Seubert, 2015). The National Aeronautics and Space Administration (NASA) JPL project Deep Space Atomic Clock (DSAC) mission aims to determine what frequency standard would fit this mission best (Ely and Seubert, 2015). An apparently good and already far-developed clock candidate for such DSAC applications is the JPL mercury trapped-ion currently in test, see Section 2.4.

4. Estimated number of SAFSs launched so far

Estimation of the accumulated GNSS-grade or better AFSs sent in space can be found in Fig. 2. We drew the separation between GNSS-grade SAFSs and others for two reasons. First, the comprehensible lack of data regarding non GNSS-grade SAFSs flown by private companies compared to publicly available pieces of information regarding GNSSs. Second, the continuum of AFSs technologies below the GNSS-grade threshold. Indeed, the use of a par-

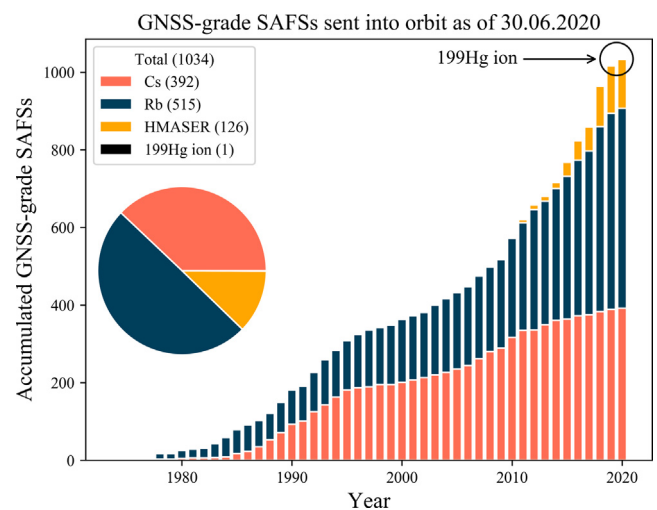


Fig. 2. Estimated number of GNSS-grade or better SAFSs sent in space as of 26 March 2020. The last database entry is the GPS-III third satellite launched 30 June 2020 (SMC Public Affairs, 2020).

ticular SAFS strongly depends on the application's specific requirements. One end of the AFS spectrum are the ground Cs fountains clocks where the principal issue is intrinsic accuracy at the price of huge volume, weight and power consumption (Sullivan et al., 2001). One other end of the spectrum are chip-scale space atomic clocks detailed in Section 5.

We estimate that at least 1034 SAFSs have been sent into orbit or deep space, the main contributor by numbers being GNSS applications. We did not count sub-orbital flights like the Gravity Probe A experiment but took into account failed and wrong orbit launches because they reflect interest in particular technologies.

It has been difficult to find pieces of information regarding some systems and we had to make reasonable assumptions. For instance, the MILSTAR satellites are said to have three or four RAFS (Mallette et al., 2006). In that particular case, we accounted three RAFS per satellite to make sure not to overestimate the real number of SAFSs sent into space.

For all years up to 1996 and 2006 we estimated at least 325 and 448 SAFSs accumulated in space compared to the 300 and 452 estimated by (Bhaskar et al., 1996) and (Mallette et al., 2006), respectively. The most sent type of SAFS (a bit less than 50%) is the RAFS followed by Cs-beam clocks, H-maser (passive and active) and finally trapped ion clock (only one reported). As of today, we estimate that the number of GNSS-grade SAFSs has more than doubled over the last 13 years. This is partially due to the rebuilding of the GLONASS constellation and the presence of two new GNSS systems, GALILEO and BeiDou. The former constellation is still being completed with new satellites whereas the latter has been completed end of June 2020 (BeiDou Navigation Satellite System, 2020).

From Fig. 2, we note a tendency to replace the Cs beam standards by passive H-masers. Therefore, the proportion of each SAFS technology has significantly changed since the 2010s.

5. Ongoing developments

In this section, we review the ongoing developments that show promising candidates for space applications such as GNSS or telecommunication. The stability performances of potential future GNSS-grade SAFSs are shown in Fig. 3.

5.1. CW-DR laser-pumped rubidium vapor cell clocks

The CW-DR laser-pumped Rb clock is very similar to the RAFS' design (Camparo, 2007). In particular, the vapor cell and the microwave cavity do not change. The discharge lamp and the filter cell are however replaced by a laser whose frequency is stabilized on one of the Rb transitions (Affolderbach et al., 2006; Vanier and Mandache, 2007). The operation mode of the clock is however the same as the lamp RAFS. The laser's narrower optical spectrum implies higher optical pumping efficiency and higher

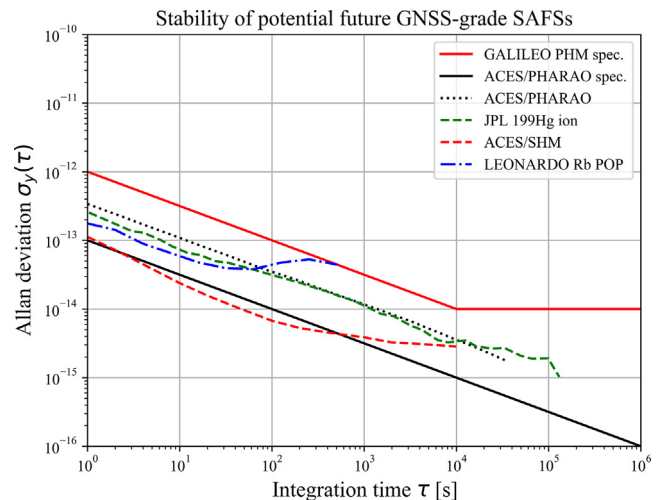


Fig. 3. Allan deviations of GNSS-grade SAFSs ongoing developments, all measured on ground. The GALILEO PHM specification is repeated as means of comparison with Fig. 1. PHARAO specifications (Sharing Earth Observation Resources, 2020), ACES/PHARAO and ACES/SHM (Laurent et al., 2015), JPL 199Hg ion (Tjoelker et al., 2016), LEONARDO Rb POP (detailed in Section 5), drift removed (Arpesi et al., 2019).

signal to noise ratio compared to the lamp RAFS resulting in an improved clock frequency stability by one order of magnitude compared to the current GNSS RAFS (Bandi et al., 2011; Gharavipour et al., 2016; Vanier and Tomescu, 2015).

The clock frequency instability is governed by the same phenomena as in the lamp RAFS (Vanier and Tomescu, 2015). In the long-term, it is also sensitive to external and operational parameters' oscillations in time (Bandi et al., 2014). Both lamp and laser-pumped vapor cell clocks exhibit frequency aging and hence stability degradation in the 10^4 s region and longer time scales, the origins of which are still not well understood but are likely to be caused by the light shift (Camparo, 2007, 2005; Formichella et al., 2017).

5.2. POP rubidium vapor-cell clocks

The physics package of the Pulsed Optically Pumped (POP) Rb clock is similar to the CW-DR laser-pumped Rb clock. Nevertheless, in the POP clock the optical and microwave interactions are separated in time (Dong et al., 2016; Kang et al., 2015; Micalizio et al., 2012). The pulsed interrogation scheme consists in applying the Ramsey's separated fields method to an atomic vapor confined in a glass cell. Following an intense optical pumping pulse, two microwave pulses separated in time are applied to the vapor cell. Finally, the clock signal is detected either via the transmission of a weak detection light or the atomic decay microwave signal is captured by the microwave cavity. The main technical difference of the POP clock compared to the CW-DR clocks is the necessity of optical and microwave

switches to realize the pulsed light for pumping (and detection) and microwave interrogation (Micalizio et al., 2010).

Both short- and long-term stabilities benefit from the use of laser and POP scheme. In the first case, Ramsey fringes result in an improved quality factor of the resonance signal compared to the CW-DR signal and better SNR. On long-term timescales, the absence of light during the two microwave pulses significantly reduces the instability contribution due to the AC Stark shift effect (also known as the light shift effect). A recent budget of long-term instabilities in such clocks however showed that residual light-induced effects still remain one of the main contributors to long term clock instability (Almat et al., 2018).

The closest industrial realization of a Rb POP clock for space applications is the LEONARDO and INRIM clock currently under development (Arpesi et al., 2019; Micalizio et al., 2019).

5.3. CPT clocks

The Coherent Population Trapping (CPT) phenomenon application is not limited to the field of AFS only (Vanier and Tomescu, 2015). In CPT clocks, the atoms are confined in a glass cell and only a bichromatic laser light is used to prepare and interrogate the atoms. The choice of atom, physics package and interrogation scheme is particularly wide and range from the continuous so-called Λ interrogation scheme of the Cs and ^{87}Rb atoms to the more exotic CPT ^{87}Rb maser and the Cs CPT-POP clock (Abdel Hafiz et al., 2018). All these implementations and associated models are described in the review by Vanier (Vanier, 2005).

The main advantage of the clocks based on the CPT approach is the absence of a microwave cavity, which makes this technique suitable for miniaturization down to chip-scale size for low power consuming clocks (Kitching, 2018; Knappe, 2007; Vanier, 2005). The interrogation is realized using two laser lights whose frequency difference coincides with the atomic transition frequency. The required multi-frequency light field can be produced by direct frequency modulation of the laser emission. Therefore, the CPT clocks require relatively more complicated optical system than the laser-pumped DR clocks described in Section 5.1.

Many miniature and Chip Scale Atomic Clock (CSAC) industrial developments such as Microsemi CPT Cs (Cash et al., 2018) and Rb (Deng et al., 2008) CSACs, AccuBeat NAC1 Rb CPT clock (Stern et al., 2016) and Symmetricom Cs MAC (Lutwak et al., 2004) target applications where small volume, low mass and low power consumption are needed and a moderate stability performance is sufficient. Typical one day time- and Allan deviations are $\leq 100 \mu\text{s}$ and 10^{-11} , respectively (Kitching, 2018). The cell's size reduction implies greater relaxation rate due to the environment and therefore degraded stability compared to the more high-performing clocks discussed above (Kitching, 2018). Although these clocks are not suitable

as GNSS standards, Space CSACs were already launched in low orbit satellites (Cash et al., 2018).

5.4. Optically-pumped Cs beam clocks

The optically-pumped Cs beam clocks employ essentially the same interrogation principle as their magnetic ancestors (Audoin and Vanier, 1989). However, in place of using magnets for atomic state selection they employ laser light to optically pump the atoms before entering the Ramsey cavity and to optically detect the clock signal at the end of it. The short-term stability (Vanier and Tomescu, 2015) is better than that of the magnetically-selected Cs beam clocks, and they are now becoming available as commercial products. The simplest design consists of using the emission of one laser source divided in two parts for state preparation by optical pumping and detection.

Development of space-grade optically-pumped Cs beam clocks have been reported for GPS (Lutwak et al., 2001), GALILEO (Lecomte et al., 2007) as well as for industrial applications (Schmeissner et al., 2016).

5.5. Cold atom clocks

In Cs fountain clocks, the primary frequency standards used for international timekeeping, the laser-cooled atoms travel vertically on a fountain-like trajectory. Thanks to the low speed of the laser-cooled atoms, very long Ramsey times and thus narrow Ramsey signal fringes and ultimate clock stability at the level of $10^{-13} \tau^{-1/2}$ or better are obtained. The first and only demonstration as of today of such SAFS in orbit is the Chinese Rb cold atom clock (CAC) (Liu et al., 2018) whose space presence is a first step towards laser-based SAFS. We already mentioned the upcoming laser-cooled Cs beam clock PHARAO in Section 3.2.3.

In view of realizing much more compact cold-atom clocks for both ground and space GNSS segments, laser-cooled atomic samples based on vapor-cell technology are envisaged. An example for this was the HORACE cold Cs clock aiming for both ground-based and in microgravity applications, in which the atoms were cooled and interrogated inside a vapor-cell-like glass container (Esnault et al., 2011). The technology was transferred to the Muquans company and a first compact cold atom clock named Rubiclock was developed based on Rb atoms. Even though the design is similar, the change from Cs to Rb was motivated by the potentially lower collision shifts (Pelle et al., 2018) and the easier realization of the required laser systems based on high-reliability telecom components. This technology is now a commercially available product aiming for ground applications (MuQuans, 2019). Another commercially available cold Rb clock is cRb-clock developed by SpectraDynamics (Ascarrunz et al., 2018). We further note the alternative approach of creating the optical molasses by means of a grating magneto-optical trap

(gMOT) shows promising results in view of its application in atomic clocks and reducing the clock's size (Elvin et al., 2019).

5.6. Other types of potential SAFS and optical lattice clocks

We have reviewed in the previous sections the most promising advances reported towards high-performance SAFS. There are many other developments ongoing on advanced technology for ground AFS or other that may also be of interest for space applications in the future whose detailed discussion is beyond the scope of this work, such as nuclear frequency standards (NFS) (Thirolf et al., 2019).

In particular, several approaches to trapped-ion clock candidates, such as Ytterbium (Mulholland et al., 2019), are under development, using different atomic species (Burt et al., 2010; DeLhay and Lacroûte, 2018; Vanier and Tomescu, 2015). Nevertheless, we should lastly mention the most stable and most accurate (Vanier and Tomescu, 2015) ground clocks so far are the optical lattice clocks (Ludlow et al., 2015). ESA foresees sending such a clock to space before “the end of the decade” (Schiller et al., 2017).

6. Conclusion

Today's GNSS constellations rely on well-established classical technologies such as the lamp-pumped Rb vapor-cell clocks, the passive H-maser and the Cs thermal-beam AFSs. The new GNSS constellations such as GALILEO and BeiDou have sent a dozen of passive H-masers in orbit, making this type of clock not only dedicated to scientific missions anymore.

Three milestones are to be noted. First, we have estimated that by mid-2020, more than 1000 SAFS have been sent in space so far. Second, the presence in orbit of the JPL mercury trapped ion clock that, as a new type of SAFS, brings the number of flying clock technologies to a total of four. Third, the in-orbit demonstration of the Chinese laser-pumped cold atom clock.

Furthermore, efforts to improve the metrological properties of the three classical SAFS technologies are still ongoing. New technologies making use of lasers are about to leave the Earth into space for scientific missions. As history has shown, it is probably only a matter of time before they are also widely used in GNSS applications and others.

Declaration of Competing Interest

The authors declare that they have no known competing financial interests or personal relationships that could have appeared to influence the work reported in this paper.

Acknowledgments

This work was supported by the University of Neuchâtel, the Swiss Space Center (UppMAC project 0720_MR_001_SSC01_00), the European Space Agency ESA (ESTEC contracts 4000129974 and 4000131046), and by the European Union's Horizon 2020 Research and Innovation Program through Quantum Technology Flagship (project macQsimal, grant 820393).

The authors thank Dr. Hartmut Schweda and Dr. Songbai Kang for helpful exchanges.

References

- Abdel Hafiz, M., Coget, G., Petersen, M., et al., 2018. Symmetric autobalanced Ramsey interrogation for high-performance coherent-population-trapping vapor-cell atomic clock 244102. *Appl. Phys. Lett.* 112. <https://doi.org/10.1063/1.5030009>.
- Affolderbach, C., Droz, F., Mileti, G., 2006. Experimental demonstration of a compact and high-performance laser-pumped Rubidium gas cell atomic frequency standard. *IEEE Trans. Instrum. Meas.* 55, 429–435. <https://doi.org/10.1109/TIM.2006.870331>.
- Akiyama, K., Alberdi, A., Alef, W., et al., 2019. First M87 event horizon telescope results. IV. Imaging the central supermassive black hole. *Astrophys. J. Lett.* 875, L4. <https://doi.org/10.3847/2041-8213/ab0e85>.
- Almat, N., Pellaton, M., Moreno, W., et al., 2018. Rb vapor-cell clock demonstration with a frequency-doubled telecom laser. *Appl. Opt.* 57, 4707. <https://doi.org/10.1364/ao.57.004707>.
- Arditi, M., Carver, T.R., 1964. Atomic clock using microwave pulse-coherent techniques. *IEEE Trans. Instrum. Meas.* IM–13, 146–152. <https://doi.org/10.1109/TIM.1964.4313389>.
- Arpesi, P., Belfi, J., Gioia, M., et al., 2019. Rubidium Pulsed Optically Pumped Clock for Space Industry. *IFCS/EFTF 2019 - Jt. Conf. IEEE Int. Freq. Control Symp. Eur. Freq. Time Forum, Proc.* 2, 1–3. <https://doi.org/10.1109/FCS.2019.8856140>
- Ascarrunz, F.G., Dudin, Y.O., Delgado Aramburo, M.C., et al., 2018. A Portable Cold 87Rb Atomic Clock with Frequency Instability at One Day in the 3 x 10⁻¹⁵ Range. *IFCS 2018 - IEEE Int. Freq. Control Symp.* 1–3. <https://doi.org/10.1109/FCS.2018.8597585>
- Astro Space Center, 2019. RadioAstron Newsletter Number 36 [WWW Document] accessed 31.03.20 http://www.asc.rssi.ru/radioastron/news/news_en.pdf, .
- Audoin, C., Vanier, J., 1989. *The Quantum Physics of Atomic Frequency Standards*, Volume 1, Bristol, England: IoP Publishing Ltd. <https://doi.org/10.1201/9781420050851.fmatt>
- Bandi, T., Affolderbach, C., Calosso, C.E., et al., 2011. High-performance laser-pumped rubidium frequency standard for satellite navigation. *Electron. Lett.* 47, 698–699. <https://doi.org/10.1049/el.2011.0389>.
- Bandi, T., Affolderbach, C., Stefanucci, C., et al., 2014. Compact high-performance continuous-wave double-resonance rubidium standard with 1.4 × 10⁻¹³ τ^{-1/2} stability. *IEEE Trans. Ultrason. Ferroelectr. Freq. Control* 61, 1769–1778. <https://doi.org/10.1109/TUFFC.2013.005955>.
- Bandi, T., Kaintura, J., Saiyed, A.R., et al., 2019. Indian Rubidium Atomic Frequency Standard (IRAFS) development for satellite navigation, in: 2019 URSI Asia-Pacific Radio Science Conference, AP-RASC 2019. Institute of Electrical and Electronics Engineers Inc. <https://doi.org/10.23919/URSIAP-RASC.2019.8738208>
- Bauch, A., 2003. Caesium atomic clocks: function, performance and applications. *Meas. Sci. Technol.* 14, 1159–1173. <https://doi.org/10.1088/0957-0233/14/8/301>.
- BeiDou Navigation Satellite System, 2020. The BDS-3 Constellation Deployment Is Fully Completed Six Months Ahead of Schedule UNOOSA Sends a Congratulation Letter [WWW Document] accessed

- 08.07.20 http://en.beidou.gov.cn/WHATSNEWS/202006/t20200623_20692.html, .
- Belyaev, A.A., Demidov, N.A., Medvedev, S.Y., et al., 2019. Russian hydrogen masers for ground and space applications. 2019 URSI Asia-Pacific Radio Sci. Conf. AP-RASC 2019 1. <https://doi.org/10.23919/URSIAP-RASC.2019.8738340>
- Betz, J.W., 2015. *Engineering satellite-based navigation and timing: global navigation satellite systems, signals, and receivers*. John Wiley & Sons, Hoboken NJ, USA.
- Bhaskar, N.D., Matt, A.D., Russo, N., et al., 1997. On-orbit performance of Milstar rubidium and quartz frequency standards. In: Proceedings of the Annual IEEE International Frequency Control Symposium. IEEE, pp. 329–337. <https://doi.org/10.1109/freq.1997.638566>.
- Bhaskar, N.D., White, J., Mallette, L.A., et al., 1996. Historical review of atomic frequency standards used in space systems. Proc. Annu. IEEE Int. Freq. Control Symp. 24–31. <https://doi.org/10.1109/freq.1996.559816>.
- Bird, M.K., Heyl, M., Allison, M., et al., 1997. The Huygens doppler wind experiment. Huygens Sci. Payload Mission. Proc. an ESA Conf. 1177, 139–162.
- Bloch, M., Mancini, O., McClelland, T., 2002. Performance of rubidium and quartz clocks in space. In: Proceedings of the Annual IEEE International Frequency Control Symposium, pp. 505–509. <https://doi.org/10.1109/freq.2002.1075936>.
- Burt, E.A., Taghavi-Larigani, S., Tjoelker, R.L., 2010. A new trapped ion atomic clock based on 201Hg^+ . IEEE Trans. Ultrason. Ferroelectr. Freq. Control, 629–635. <https://doi.org/10.1109/TUFFC.2010.1458>.
- Burt, E.A., Yi, L., Tucker, B., et al., 2016. JPL ultrastable trapped ion atomic frequency standards. IEEE Trans. Ultrason. Ferroelectr. Freq. Control 63, 1013–1021. <https://doi.org/10.1109/TUFFC.2016.2572701>.
- Camparo, J., 2005. Does the light shift drive frequency aging in the rubidium atomic clock? IEEE Trans. Ultrason. Ferroelectr. Freq. Control 52, 1075–1078. <https://doi.org/10.1109/TUFFC.2005.1503993>.
- Camparo, J., 2007. The rubidium atomic clock and basic research. Phys. Today 60, 33–39. <https://doi.org/10.1063/1.2812121>.
- Cash, P., Krzewick, W., MacHado, P., et al., 2018. Microsemi Chip Scale Atomic Clock (CSAC) technical status, applications, and future plans. In: 2018 European Frequency and Time Forum, EFTF 2018. Institute of Electrical and Electronics Engineers Inc., pp. 65–71. <https://doi.org/10.1109/EFTF.2018.8408999>
- Couplet, C., Rochat, P., Mileti, G., et al., 1995. Miniaturized rubidium clocks for space and industrial applications. In: Proceedings of the Annual IEEE International Frequency Control Symposium. IEEE, pp. 53–59. <https://doi.org/10.1109/freq.1995.483882>.
- Dehmelt, H., 1990. Experiments with an isolated subatomic particle at rest (Nobel Lecture). *Angew. Chemie Int. Ed. English* 29, 734–738.
- Delehay, M., Lacroûte, C., 2018. Single-ion, transportable optical atomic clocks. J. Mod. Opt. 65, 622–639. <https://doi.org/10.1080/09500340.2018.1441917>.
- Delva, P., Puchades, N., Schönemann, E., et al., 2019. A new test of gravitational redshift using Galileo satellites: The GREAT experiment. *Comptes Rendus Phys.* 20, 176–182. <https://doi.org/10.1016/j.crhy.2019.04.002>.
- Deng, J., Vltas, P., Taylor, D., et al., 2008. A commercial CPT rubidium clock. EFTF 2008 - 22nd Eur. Freq. Time Forum 99.
- Department of Space Indian Space Research Organisation, n.d. List of Navigation Satellites [WWW Document]. URL <https://www.isro.gov.in/spacecraft/list-of-navigation-satellites> (accessed 30.03.20).
- Dong, G., Deng, J., Lin, J., et al., 2016. The progress of pulsed optically pumped rubidium clock at SIOM. 2016 Prog. Electromagn. Res. Symp. PIERS 2016 - Proc. i, 3716–3719. <https://doi.org/10.1109/PIERS.2016.7735410>.
- Droz, F., Mosset, P., Barmaverain, G., et al., 2006. The on-board Galileo clocks: Rubidium standard and passive hydrogen maser - Current status and performance. Proc. 20th Eur. Freq. Time Forum, EFTF 2006, 420–426.
- Droz, F., Mosset, P., Wang, Q., et al., 2009. Space passive hydrogen maser - Performances and lifetime data. 2009 IEEE Int. Freq. Control Symp. Jt. with 22nd Eur. Freq. Time Forum, 393–398. <https://doi.org/10.1109/FREQ.2009.5168208>.
- Elvin, R., Hoth, G.W., Wright, M., et al., 2019. Cold-atom clock based on a diffractive optic. *Opt. Express* 27, 38359. <https://doi.org/10.1364/oe.378632>.
- Ely, T.A., Seubert, J., 2015. One-way radiometric navigation with the Deep Space Atomic Clock. Proc. AAS/AIAA Sp. Flight Mech. Meet, pp. 1–18.
- Esnault, F.X., Rossetto, N., Holleville, D., et al., 2011. HORACE: A compact cold atom clock for Galileo. *Adv. Sp. Res.* 47, 854–858. <https://doi.org/10.1016/j.asr.2010.12.012>.
- Essen, L., Parry, J.V.L., 1955. An atomic standard of frequency and time interval: A caesium resonator. *Nature* 176, 280–282. <https://doi.org/10.1038/176280a0>.
- European GNSS Agency, 2020. Constellation Information [WWW Document] accessed 30.03.20 <https://www.gsc-europa.eu/system-service-status/constellation-information>, .
- European Space Agency, 2018. Extended life for ESA's science missions [WWW Document] accessed 04.04.20 <https://sci.esa.int/web/director-desk/-/60943-extended-life-for-esas-science-missions#1>, .
- FEI, 2013. FEI's Next-Generation Rubidium Atomic Frequency Standard For Space Applications. New York, USA. Available online at <https://freleec.com/wp-content/uploads/2019/03/4-RAFS-Brochure.pdf> (accessed 30.03.20)
- Formichella, V., Camparo, J., Tavella, P., 2017. Influence of the ac-Stark shift on GPS atomic clock timekeeping 043506. *Appl. Phys. Lett.* 110. <https://doi.org/10.1063/1.4975071>.
- Georgescu, I., 2019. A space chronometer. *Nat. Rev. Phys.* 1, 421–421. <https://doi.org/10.1038/s42254-019-0084-9>
- Gharavipour, M., Affolderbach, C., Kang, S., et al., 2016. High performance vapour-cell frequency standards. *J. Phys. Conf. Ser.* 723. <https://doi.org/10.1088/1742-6596/723/1/012006> 012006.
- Gill, P., 2005. Optical frequency standards. *Metrologia* 42, S125–S137. <https://doi.org/10.1088/0026-1394/42/3/S13>.
- Gill, P., Barwood, G.P., Klein, H.A., et al., 2003. Trapped ion optical frequency standards. *Meas. Sci. Technol.* 14, 1174. <https://doi.org/10.1088/0957-0233/14/8/302>.
- Guo, M., Fan, Y., Fan, X., et al., 2020. Performance analysis of BDGIM. In: China Satellite Navigation Conference. Springer, pp. 101–113. https://doi.org/10.1007/978-981-15-3715-8_10.
- Hafele, J.C., Keating, R.E., 1972. Around-the-world atomic clocks: Predicted relativistic time gains. *Science* (80-) 177, 166–168. <https://doi.org/10.1126/science.177.4044.166>.
- Heß, M.P., Stringhetti, L., Hummelsberger, B., et al., 2011. The ACES mission: System development and test status. *Acta Astronaut.* 69, 929–938. <https://doi.org/10.1016/j.actaastro.2011.07.002>.
- Huang, G., Cui, B., Zhang, Q., et al., 2019. Switching and performance variations of on-orbit BDS satellite clocks. *Adv. Sp. Res.* 63, 1681–1696. <https://doi.org/10.1016/j.asr.2018.10.047>.
- ISS-Reshetnev, 2020. News [WWW Document]. URL <http://www.iss-reshetnev.com/media/news/> (accessed 30.03.20).
- Kang, S., Gharavipour, M., Affolderbach, C., et al., 2015. Demonstration of a high-performance pulsed optically pumped Rb clock based on a compact magnetron-type microwave cavity. *J. Appl. Phys.* 117, 19–23. <https://doi.org/10.1063/1.4914493>.
- Kardashev, N.S., Khartov, V.V., Abramov, V.V., et al., 2013. “Radio-Astron”—A telescope with a size of 300 000 km: Main parameters and first observational results. *Astron. Reports* 57, 153–194. <https://doi.org/10.1134/S1063772913030025>.
- Kitching, J., 2018. Chip-scale atomic devices. *Appl. Phys. Rev.* 5, 31302. <https://doi.org/10.1063/1.5026238>.
- Knappe, S.A., 2007. MEMS atomic clocks. In: Gianchandani, Y.B., Tabata, O., Zappe, H. (Eds.), *Comprehensive Microsystems*. Elsevier, Amsterdam, NL, pp. 571–612.

- Laurent, P., Abgrall, M., Clairon, A., et al., 2007. The space program PHARAO/ACES, in: Time and Frequency Metrology. International Society for Optics and Photonics, p. 667308.
- Laurent, P., Massonnet, D., Cacciapuoti, L., et al., 2015. The ACES/PHARAO space mission. *Comptes Rendus Phys.* 16, 540–552. <https://doi.org/10.1016/j.crhy.2015.05.002>.
- Lecomte, S., Haldimann, M., Ruffieux, R., et al., 2007. Performance demonstration of a compact, single optical frequency cesium beam clock for space applications. *Proc. IEEE Int. Freq. Control Symp. Expo.* 1127–1131. <https://doi.org/10.1109/FREQ.2007.4319254>
- Liu, L., Lü, D.S., Chen, W.B., et al., 2018. In-orbit operation of an atomic clock based on laser-cooled 87Rb atoms. *Nat. Commun.* 9, 2760. <https://doi.org/10.1038/s41467-018-05219-z>.
- Lockheed Martin, 2020. Protected Globally: AEHF-6 Satellite Actively Communicating With U.S. Space Force [WWW Document]. URL https://news.lockheedmartin.com/AEHF6_satellite_successfully_launched?_ga=2.65465959.810220687.1593614164-2042781626.1583256981 (accessed 01.07.20).
- Los Angeles Air Force Base, 2012a. GPS IIF [WWW Document] accessed 30.03.20 <https://www.losangeles.af.mil/About-Us/Fact-Sheets/Article/343724/gps-iif/>, .
- Los Angeles Air Force Base, 2012b. GPS III [WWW Document] accessed 30.03.20 <https://www.losangeles.af.mil/About-Us/Fact-Sheets/Article/343728/gps-iii/>, .
- Ludlow, A.D., Boyd, M.M., Ye, J., et al., 2015. Optical atomic clocks. *Rev. Mod. Phys.* 87, 637–701. <https://doi.org/10.1103/RevModPhys.87.637>.
- Lutwak, R., Deng, J., Riley, W., et al., 2004. The chip-scale atomic clock – low-power physics package. In: *Proceedings of the 36th Precise Time and Time Interval (PTTI) Systems and Applications Meeting*, p. 33.
- Lutwak, R., Emmons, D., Garvey, R.M., et al., 2001. Optically Pumped Cesium-Beam Frequency Standard for Gps-Iii. 33rd Annu. Precise Time Time Interval Meet. 19–32.
- Maleki, L., Prestage, J., 2005. Applications of clocks and frequency standards: from the routine to tests of fundamental models. *Metrologia* 42, S145. <https://doi.org/10.1088/0026-1394/42/3/S15>.
- Mallette, L.A., Rochat, P., White, J., 2006. Historical review of atomic frequency standards used in space systems - 10 year update, in: 38th Annual Precise Time and Time Interval (PTTI) Systems and Applications Meeting 2006. pp. 69–80.
- Mallette, L.A., White, J., Rochat, P., 2010. Space qualified frequency sources (clocks) for current and future GNSS applications. *Rec. - IEEE PLANS, Position Locat. Navig. Symp.*, 903–908 <https://doi.org/10.1109/PLANS.2010.5507225>.
- Mallette, L.A., Rochat, P., White, J., et al., 2012. Space Qualified Frequency Sources (Clocks) for GNSS Applications : 2012 Update, in: *Joint Navigation Conference 2012*. Available online at <https://www.researchgate.net/publication/311667882> (accessed 30.04.20)
- McCaskill, T.B., Buisson, J.A., 1975. NTS-1 (TIMATION III) Quartz-and Rubidium-Oscillator Frequency-Stability Results, in: *Proceedings of the 29th Annual Symposium on Frequency Control*. NAVAL RESEARCH LAB WASHINGTON DC, pp. 425–435.
- McCaskill, T.B., White, J., Stebbins, S., et al., 1978. NTS-2 cesium frequency stability results. *Proc. 32nd Annu Symp. Freq. Control* 1978, 560–566. <https://doi.org/10.1109/freq.1978.200290>.
- Mei, G., Zhong, D., An, S., et al., 2016. Main features of space rubidium atomic frequency standard for BeiDou satellites. 2016 Eur. Freq. Time Forum, EFTF 2016 0–3. <https://doi.org/10.1109/EFTF.2016.7477803>
- Micalizio, S., Calosso, C.E., Godone, A., et al., 2012. Metrological characterization of the pulsed Rb clock with optical detection. *Metrologia* 49, 425–436. <https://doi.org/10.1088/0026-1394/49/4/425>.
- Micalizio, S., Calosso, C.E., Levi, F., et al., 2019. Preliminary characterization of a rb pulsed optically pumped clock for space applications. 2019 IEEE Int. Work. Metrol. AeroSpace, Metroaerosp. 2019 - Proc. 682–686. <https://doi.org/10.1109/MetroAeroSpace.2019.8869595>
- Micalizio, S., Godone, A., Levi, F., et al., 2010. Pulsed optically pumped Rb clock with optical detection: first results. *European Frequency and Time Forum. IEEE*, pp. 1–8.
- Microsemi, 2020. 5071A - Cesium Clock Primary Frequency Standard [WWW Document]. URL <https://www.microsemi.com/product-directory/cesium-frequency-references/4115-5071a-cesium-primary-frequency-standard> (accessed 06.04.20).
- Mulholland, S., Klein, H.A., Barwood, G.P., et al., 2019. Laser-cooled ytterbium-ion microwave frequency standard. *Appl. Phys. B* 125, 198. <https://doi.org/10.1007/s00340-019-7309-6>.
- MuQuans, 2019. MuClock: A high-performance frequency standard based on cold atoms [WWW Document]. URL https://www.muquans.com/wp-content/uploads/2019/03/muquans_muclock.pdf (accessed 30.04.20).
- Nakamura, M., Takahashi, Y., Amagai, J., et al., 2011. Time management system of the QZSS and time comparison experiments, in: 29th AIAA International Communications Satellite Systems Conference (ICSSC-2011). p. 8067.
- Peil, S., Swanson, T.B., Hanssen, J., et al., 2017. Microwave-clock timescale with instability on order of 10^{-17} . *Metrologia* 54, 247.
- Pelle, B., Szmuk, R., Desruelle, B., et al., 2018. Cold-Atom-Based Commercial Microwave Clock at the 10–15 Level. *IFCS 2018 - IEEE Int. Freq. Control Symp.* 1–5. <https://doi.org/10.1109/FCS.2018.8597468>
- Prusti, T., De Bruijne, J.H.J., Brown, A.G.A., et al., 2016. The gaia mission. *Astron. Astrophys.* 595, A1. <https://doi.org/10.1051/0004-6361/201629272>.
- Quasi-Zenith Satellite System, 2020. List of Positioning Satellites [WWW Document] accessed 30.03.20 <https://qzss.go.jp/en/technical/satellites/index.html#QZSS>, .
- Ramsey, N.F., 1956. Thermodynamics and statistical mechanics at negative absolute temperatures. *Phys. Rev.* 103, 20.
- Ramsey, N.F., 1990. Experiments with separated oscillatory fields and hydrogen masers. *Science (80-)* 248, 1612–1619.
- Riehle, F., 2003. *Frequency Standards: Basics and Applications*. Wiley-VCH, Weinheim, DE. <https://doi.org/10.1002/3527605991>.
- Riehle, F., Gill, P., Arias, F., et al., 2018. The CIPM list of recommended frequency standard values: guidelines and procedures. *Metrologia* 55, 188. <https://doi.org/10.1088/1681-7575/aaa302>.
- Rochat, P., Schweda, H., Mileti, G., et al., 1994. Developments of rubidium frequency standards at Neuchatel observatory. In: *Proceedings of IEEE 48th Annual Symposium on Frequency Control*. IEEE, pp. 716–723.
- Schiller, S., Lemonde, P., Tino, G.M., et al., 2017. The space optical clocks project. In: Kadowaki, N. (Ed.), *International Conference on Space Optics — ICSO 2010*, 47. SPIE. <https://doi.org/10.1117/12.2309166>
- Schmeissner, R., Douahi, A., Barberau, I., et al., 2016. Towards an engineering model of optical space Cs clock. 2016 Eur. Freq. Time Forum, EFTF 2016 3–6. <https://doi.org/10.1109/EFTF.2016.7477843>
- Seubert, J., Ely, T., Prestage, J., et al., 2013. The deep space atomic clock: ushering in a new paradigm for radio navigation and science. *Adv. Astronaut. Sci.* 148, 1851–1865.
- Sharing Earth Observation Resources, 2020. ISS Utilization: ACE (Atomic Clock Ensemble in Space) [WWW Document] accessed 30.03.20 <https://earth.esa.int/web/eoportal/satellite-missions/i-iss-aces>, .
- SMC Public Affairs, 2020. SMC and its partners successfully launch third GPS III satellite [WWW Document] accessed 06.07.20 <https://www.losangeles.af.mil/News/Article-Display/Article/2243339/smc-and-its-partners-successfully-launch-third-gps-iii-satellite/>, .
- Stern, A., Levy, B., Levy, C., et al., 2016. The NAC-a miniature CPT Rubidium clock. In: 2016 European Frequency and Time Forum (EFTF). IEEE, pp. 1–4.
- Sullivan, D.B., Bergquist, J.C., Bollinger, J.J., et al., 2001. Primary atomic frequency standards at NIST. *J. Res. Natl. Inst. Stand. Technol.* 106, 47.

- Teunissen, P., Montenbruck, O. (Eds.), 2017. Springer Handbook of Global Navigation Satellite Systems. Springer International Publishing, Cham, CH. <https://doi.org/10.1007/978-3-319-42928-1>
- Thirolf, P.G., Seiferle, B., von der Wense, L., 2019. The 229-thorium isomer: doorway to the road from the atomic clock to the nuclear clock. *J. Phys. B At. Mol. Opt. Phys.* 52, 203001.
- Thoelert, S., Montenbruck, O., Meurer, M., 2014. IRNSS-1A: signal and clock characterization of the Indian regional navigation system. *GPS Solut.* 18, 147–152.
- Tjoelker, R.L., Prestage, J.D., Burt, E.A., et al., 2016. Mercury ion clock for a NASA technology demonstration mission. *IEEE Trans. Ultrason. Ferroelectr. Freq. Control* 63, 1034–1043. <https://doi.org/10.1109/TUFFC.2016.2543738>.
- Utkin, A., Belyaev, A., Pavlenko, Y., et al., 2012. On-Board active hydrogen maser for RADIOASTRON mission (design and experimental results) Parameters of the Orbit. 6th Int. Symp. “METROLOGY TIME SPACE”. Available online at <http://www.vremya-ch.com/english/materials/files/utkin.pdf> (accessed 30.04.20)
- Vanier, J., 2005. Atomic clocks based on coherent population trapping: A review. *Appl. Phys. B Lasers Opt.* <https://doi.org/10.1007/s00340-005-1905-3>
- Vanier, J., Audoin, C., 2005. The classical caesium beam frequency standard: fifty years later. *Metrologia* 42, S31. <https://doi.org/10.1088/0026-1394/42/3/S05>.
- Vanier, J., Mandache, C., 2007. The passive optically pumped Rb frequency standard: The laser approach. *Appl. Phys. B Lasers Opt.* 87, 565–593. <https://doi.org/10.1007/s00340-007-2643-5>.
- Vanier, J., Tomescu, C., 2015. *The Quantum Physics of Atomic Frequency Standards: Recent Developments*. CRC Press, Boca Raton FL, USA.
- Vessot, R.F.C., Levine, M.W., Mattison, E.M., et al., 1980. Test of relativistic gravitation with a space-borne hydrogen maser. *Phys. Rev. Lett.* 45, 2081–2084. <https://doi.org/10.1103/PhysRevLett.45.2081>.
- Waller, P., Gonzalez, F., Binda, S., et al., 2009. Update on the in-orbit performances of GIOVE clocks. In: 2009 IEEE International Frequency Control Symposium Joint with the 22nd European Frequency and Time Forum, pp. 388–392. <https://doi.org/10.1109/FREQ.2009.5168207>.
- Wu, Z., Zhou, S., Hu, X., et al., 2018. Performance of the BDS3 experimental satellite passive hydrogen maser. *GPS Solut.* 22. <https://doi.org/10.1007/s10291-018-0706-1>.
- Wynands, R., Weyers, S., 2005. Atomic fountain clocks. *Metrologia* 42, S64. <https://doi.org/10.1088/0026-1394/42/3/S08>.
- Xu, X., Wang, X., Liu, J., et al., 2019. Characteristics of BD3 global service satellites: POD, open service signal and atomic clock performance. *Remote Sens.* 11, 1–17. <https://doi.org/10.3390/rs11131559>.